doi:10.3166/acsm.40.43-50 © Lavoisier, Paris
Gold flower-shape crystals *Ann. Chim. Sci. Mat.*, 2016, 40 (1-2), pp. 43-50

OPTICAL AND ELECTROCHEMICAL ACTIVITY OF GOLD FLOWER-SHAPE CRYSTALS

Pierre BAUER[a], Karine MOUGIN[a], Vincent VIGNAL[b], Halina KRAWIEC[c], Mohammad RAJAB[a], Arnaud BUCH[d], Pierre PONTHIAUX[d], Delphine FAYE[e]

[a] Institut de Science des Matériaux de Mulhouse, UMR 7361 CNRS-Université de Haute Alsace, 15 Rue Jean Starcky, BP 2488, 68057 Mulhouse cedex, France.
[b] Laboratoire Interdisciplinaire Carnot de Bourgogne, UMR 6303 CNRS-Université de Bourgogne, 9 avenue Alain Savary, BP 47870, 21078 Dijon cedex, France.
[c] Laboratoire Interdisciplinaire Carnot de Bourgogne, UMR 6303 CNRS-Université de Bourgogne, 9 avenue Alain Savary, BP 47870, 21078 Dijon cedex, France.
[d] AGH-University of Science and Technology, Faculty of Foundry Engineering, Reymonta 23 street, 30-059 Krakow, Poland.
e Centre Nationale d'Etudes Spatiales, 18 Avenue Édouard Belin, 31400 Toulouse, France

Abstract – A novel approach for a controlled growth of pattern-directed organization of Au flower shape crystals (NFS) onto rigid substrate has been proposed to achieve large-scale functional materials. This process is based on the combination of soft nanoporous template and a multistage aqueous chemical method. First, a hexagonal array of gold nanoparticles was prepared using a nanoporous thin membrane by a seed-mediated growth colloidal process. The size and morphology of the Au NFs were then controlled by a site selective heterogeneous nucleation and growth onto the Au precursors. The growth mechanism of the template-directed synthesis of Au crystals arrays was investigated. The optical and electrochemical properties of Au NFs were discussed in relation with their morphology and organization. Results show that the nature, the size, the interparticle distance and their density strongly affect the intensity of the optical and electrochemical signals. Finally, this easy and multistep approach is particularly attractive due to its environmentally gentle processing conditions and represents an open pathway to several large-scale nanomaterials fabrication.

Résumé – Réseau de nanofleurs d'or : synthèse et propriétés optiques et électrochimiques. Une nouvelle approche d'assemblage dirigé de nanofleurs d'or (NFs) structurées sur substrats rigides a été proposée et, ce dans le but, de développer une technique permettant une structuration à grande échelle. Ce procédé combine le dépôt et l'auto-assemblage d'un film mince de copolymère et un procédé chimique de réduction douce de sels métalliques en milieux aqueux. La première étape consiste à réaliser un réseau hexagonal de nanoparticules d'or par réduction chimique dans les nanopores du copolymère. Ensuite, la croissance *in-situ* de NFs d'or a été réalisée sur cette préstructuration. Le mécanisme de croissance de ces nanofleurs a été étudié. Les analyses de surface montrent que la nature, la taille, la distance interparticule, et la densité des NFs affectent fortement la réponse optique et électrochimique de ce système. Finalement, cette technique de structuration

Tirés-à-part : K.MOUGIN, IS2M, CNRS-Université de Haute Alsace, 68057 Mulhouse, France.

de surface simple et écologique représente une ouverture vers la structuration des nanomatériaux à grande échelle et, en particulier, pour des applications dans le domaine des nanodétecteurs.

1. INTRODUCTION

Metallic nanostructures have been the subject of intensive scientific researches due to their fascinating physical and chemical properties and their relevant applications in optics [1], catalysts and photonics [2], in surface-enhanced Raman scattering (SERS) or as chemical sensors [3,4]. All these applications are influenced by the size, shape and morphology of metallic nanostructures [5]. Nowadays, nanospheres [6], nanotubes [7], nanoplates [8], nanocubes [9] or nanorods [10] have been synthesized by a variety of methods. The possibility of formation of various nanoforms frequently depends on the synthesis conditions and today, the conditions for common forms are well-known. But a class of sophisticated flower-like or dendritic structures have been generated recently. Nanoflowers (NFs) are not so currently reported as this complicated morphology leads to several difficulties in forming well-defined dendritic nanostructures [11]. Various methods have been developed to fabricate dendritic noble metal nanostructures such as electrodeposition[12], photochemical way [13], wet chemical method [14], seeded growth method [15], hydrothermal reduction [16] or a template method [17]. For instance, Wang and co-workers have reported successful synthesis of five-star gold nanostructures in aqueous solution via the use of a structuring agent [18, 19, 20]. Huang and his team has reported the preparation of three- dimensional dendritic gold nanostructures with various capping agents in solution [21]. However, the quality of these nanoflowers grown in water in terms of size, shape and especially distribution is significantly low. The seeding approach to the synthesis of larger colloidal Au nanoparticles offers an alternative to obtain an improved monodispersity relative to the Frens method. In order to control the nucleation density, the orientation and the crystalline phase, different approaches can be used. Recently, Möller and co-workers successfully prepared uniform gold nanoparticles and arranged them spatially in 2D arrays by using polystyrene-b-poly(2-vinylpyridine) (PS-P4VP) diblock copolymer micelles [24]. This process has been also taken up by in literature by Dai and co-workers and we decide to use it also for the structuration of Au nulei.

Among the metallic nanoparticles (NPs), gold and silver NPs can exhibit rich localized surface Plasmon resonance properties, ideal for application in plasmonics and as biosensors. In addition, the great potential of multi-branched nanoparticles was shown to arise very sharp tips leading to large local field enhancement and a high surface area. Most of studies consider the optimization of the morphology of nanostructure to improve the optical or electrochemical behaviour of substrates without considering the effect of ordered arrangement of the nanostructures at micro scale. Zhang et *al.* have measured the Raman intensity of aligned Ag nanorods in relation with the interparticle distance [28]. The fluctuation of Raman signals reflects that this enhancement is obviously lattice dependent and is due to the enhancement of the localized electrical field [29].

Furthermore in the literature, electrochemical experiments have also been previously used to detect and quantify targeted molecules. However, the use of nanoflower-like sensors remains relatively scarce [30]. Lu and co-workers have made preliminary work by developing an enhanced electrochemiluminescence sensor for detecting a specific molecule [31]. They have tried to link the chemical redox reactions at the surface of gold NFs with the corresponding electrochemical signal. Some other more regular processes such as the technique of selective chemisorptions on self-assembled monolayers were also used by Youn et *al* [32]. Their active plateform was made of nanowire arrays. These preliminary results are quite encouraging and should strengthen the potential of the active flower-like pattern active surface.

In this study, we have developed a facile and efficient method to synthesize and organize Au gold nanoflowers by a site selective Au heterogeneous nucleation onto the substrate followed by a second growth onto the Au precursors. At optimized conditions, gold nanocrystals with controlled

symmetries are formed, and the control of parameters of reaction (pH, immersion time, temperature, concentration of gold salts...) has allowed us to better understand the mechanism of formation of flowers. All the samples have been prepared on stainless steel substrates and characterized by electrochemical and optical measurements to investigate the influence of the morphology and density of Au NFs onto the optical and electrical signals.

2. EXPERIMENTAL

The multistep synthesis of nanostructured films has started with the stainless steel substrate surface preparation for heterogeneous nucleation of colloidal gold nanocrystals. Then, the polymer selected for the soft template was a poly(styrene-b-4-vinyl pyridine) diblock copolymer. Thin films of this diblock copolymer (BCP) mixed with 2-(4-hydroxyphenylazo)benzoic acid (HABA) into chloroform were deposited by dip-coating over a large area onto cleaned stainless steel surface. The thickness of the dip-coated film onto the surface was of 45 ±2 nm, measured by ellipsometry. The (PS-P4VP + HABA) phase separation was then enhanced by a 4 days solvent annealing in saturated vapor of 1,4-dioxane. HABA was then removed by dipping the substrate in a methanol bath for 5 min and dried under a nitrogen flow. The nanoporous film sample was placed under UV light (λ = 254nm) for 30 min in order to strengthen the mask against hydrolysis, but also to stabilize it along the time. A plasma treatment is used (power: 90W, pressure: 1mbar) during 60s to start burning residues of HABA or P4VP coating at the bottom of the nanopores.

2.1. Gold Seeds deposition

Golden salt was added to the copolymer by immersing the BCP template film in 1% aqueous solution for 1 hour. During this adsorption step, the tetrachloroauric acid salt was reduced by the addition of a solution of hydrazine hydrate [33].

2.2. Seed-Mediated Growth of gold nanoflowers

The growth of nanoflowers is achieved by a chemical process over the Au seeds patterning deposited on the substrate. The reductant used here is a 20 mM hydroxylamine solution (NH_2OH). The samples were immersed in a hydroxylamine solution for 45 min. Then, the gold source is added (at required concentration) in small proportion (50µL) without stirring during 1 hour. The overwhole experiment is performed at room temperature at a constant pH.

2.3. Characterization

The atomic force microscopy images of the BCP and hybrid films were performed using the Bruker scanning probe microscope –multimode equipped with a nanoscope V controller in Tapping Mode ™. The AFM scans were interpreted using the Nanoscope Analysis software.
Film thicknesses were determined by null-ellipsometry (Multiskop, Optrel, Berlin, German. The microstructures of the samples and the metallic crystals morphology were investigated by high resolution scanning electron microscopy (MEB XL30 FEG, PHILIPS) at an accelerating voltage of 12 kV.

3. RESULTS

The selective growth of metallic nanostructures on a structured substrate and, particularly inside the pores of a polymer template, have been investigated. This multistep synthesis of a nanostructured hybrid film has started with the substrate surface patterning required for the heterogeneous nucleation of oriented metallic nanocrystals. Topographic AFM image of the

copolymer PS-P4VP template coated on cleaned silicon surface (*Figure 1a*) shows, after removal of the HABA, a hexagonal arrangement of cylindrical nanoholes.

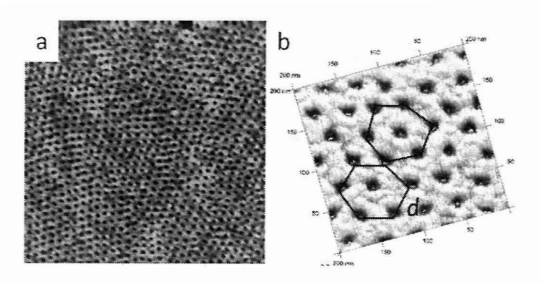

Figure 1. AFM image and 3D AFM image of the nanostructured copolymer PS-P4VP template deposited on a clean silicon surface and after annealing under solvent vapour for 3 days.

The film thickness onto stainless steel is of ~ 37± 2 nm. The AFM image in *Figure 1a* presents ordered domains that also exhibit hexagonal packing. Figure 1b shows a center-to-center distance *d* between two nanopores of 20 ± 3 nm. A chemical seeded-process was adopted to grow Au nanoparticles into the pores. The aim of this first step was to prepare small spherical gold seeds with dimensions of the order of 10 nanometers (or less).

The second stage involves the growth, from the preformed seeds, of anisotropic Au particles and/or microcrystals. The growth of gold flowers has been initiated onto Au nuclei array prepared by the facile chemical approach as described in paragraph 2.2. The substrate was covered with a large-scale Au flower-like structures arrays (*figure 2*).

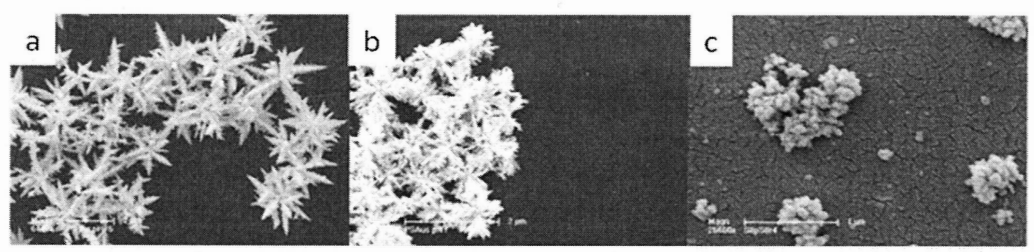

Figure 2. SEM images of gold NFs deposited on a substrate coated with a thin film of PS-P4VP. The samples have been prepared at three different pH of growth solutions (a) pH = 5, (b) pH = 6, (c) pH = 7. Scale bare 2µm.

3.1. Investigation of the pH effect onto the growth Au crystal solution

Gold crystals were obtained by a one-pot synthesis made of chemical reduction of Au ions and the use of a structuring agent such as hydroxylamnine. This facile chemical deposition approach allows the formation of metallic flower shaped structures with a size of the order of 2 µm. However, results have shown that the pH of the Au NFs growth solution has a strong impact on the morphology of the resulting crystals. Three different pH have been first investigated: a slight acidic one pH=5 (Fig. 2a), a more neutral one pH=7 (Fig. 2b) and a slight basic one pH=9 (Fig. 2c). By varying the pH growth solution, we can observe a variation of the morphology of the flowers from a more dendritic shape at slightly acidic pH, to a more arborescent morphology at a neutral pH up to a more spherical one at basic pH. This morphology change can be explained by the Cl^- ions content in the growth solution. When the Cl^- ions concentration is high, quasi-sperical Au particles are obtained. This mechanism is explained by the fact that Au atoms can move from one facet to another facet of the Au crystals in an intraparticle route. Chlorine ions bind easily to gold ions or

atoms and then facilitate their movement. Hence, the addition of a stronger ligand decreases the ripening effect of the hydroxylamine [34]. However, the fundamental mechanisms controlling Au growth on existing Au seeds is not yet well unsderstood.

To optimize the synthesis of more arborescent flower crystals, three growth solutions with a pH varying between 5 and 6 have been prepared. *Figure 3* represents the SEM images of well-defined flower-like structures for each pH of growth solution. The crystal diameter is around 2µm and the interparticle spacing is also very similar for each 3 different pH.

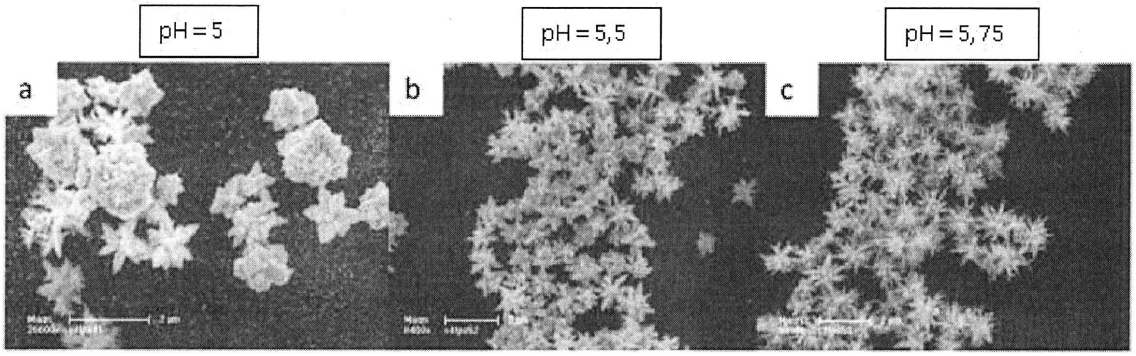

Figure 3. SEM images of gold NFs desposited onto susbtrate coated with a thin film of PS-P4VP. The samples have been prepared at three different pH of growth solutions (a) pH = 5, (b) pH = 5.5, (c) pH = 5.75. Scale bare 2µm.

3.2. Effect of the Au NFs morphology on the SERS activity

We have tested the performance of the hybrid nanostructured film covered by Au NFs by Surface-Enhanced Raman Spectroscopy (SERS) using methylen blue (MB) as the probe molecule. The adsorption of very small amounts of MB molecules was both deposited onto Au NFs structures as well as Au aggregates as the optical properties of metallic NPs strongly depend on their shape and size [35].

Prior to SERS measurement, 10^{-7} M of MB solution was prepared, and both the Au NFs and aggregates deposited onto substrates were immersed for one minute in the diluted solution, and then dried in air. Typical SERS spectra of methylen blue adsorbed onto respectively Au flower-like structures and aggregates structures are displayed in Figure 4.

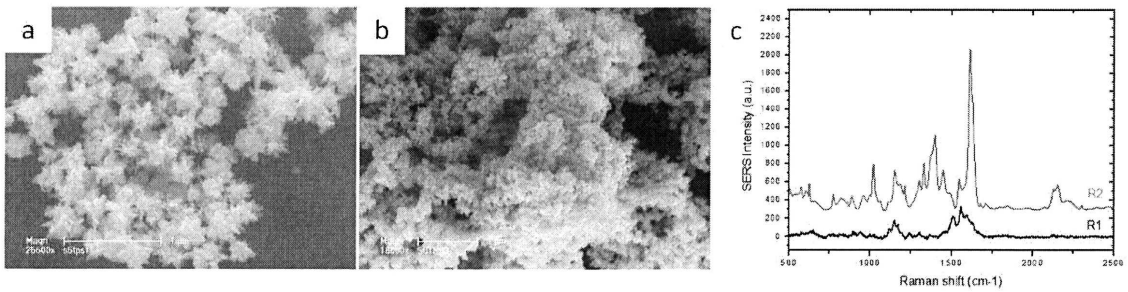

Figure 4. SEM images and SERS spectra of gold nanostructures: SEM images of (a) gold nanoflowers and (b) gold aggregated nanoparticles deposited on steel substrate coated with a thin film of PS-P4VP. (c) SERS spectra of Methylen Blue at a very low concentration (10^{-7} M) adsorbed on gold nanoflowers (R2) and gold aggregated nanoparticles (R1).

We do observe the enhancement of the Raman signal obtained by the NFs structures compared to the one of the aggregated particles. The main peak of the SERS spectra at 1623 cm^{-1} corresponds to the ring stretch modes of (*(ν*C-C*)* and *(ν*C-N-C)) of the aromatic ring of MB. The SERS enhancement factor of this peak between the flower-like and aggregated structures is of the order of 100 for equivalent methylen blue concentration. This enhancement of the signal can be explained by the enhanced electromagnetic field resulting from i) the possibility of coupling between the sharp tips at the end of each individual branch of the flowers, ii) a high surface area of the flower and iii) the possibility of coupling between the discrete and close-packed Au NFs altogether. Finally this result particularly emphasizes the fact that Au Nanoflowers crystals represent ideal SERS candidates because of the abundance of "hot spots" generated by their specific surface topography.

3.3. Effect of the Au NFs morphology on the electrochemical activity

The electrochemical activity of the structured substrates was performed with the use of a 250 µm diameter microcell. The working electrode was the substrate, a Ag/AgCl electrode as a reference and the counter electrode was a Pt wire. The aqueous medium was a solution of Na2SO4 (0.1M) and the voltamperograms were recorded at a velocity of 500 mV/sec, over 10 cycles.

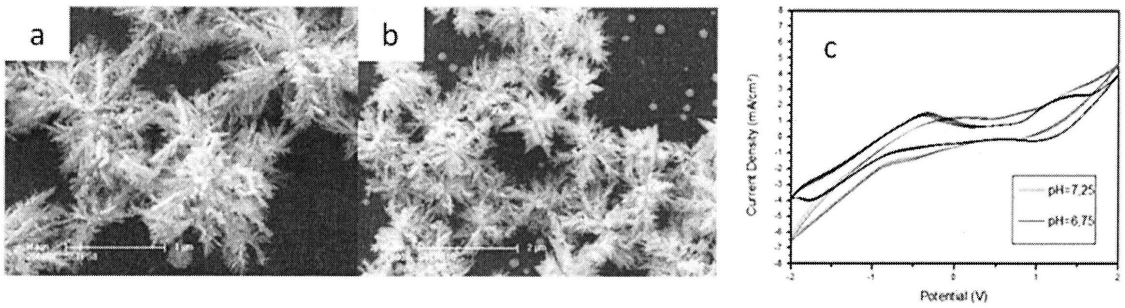

Figure 5. SEM images and cyclic voltammogram of gold nanoflowers: SEM images of gold nanoflowers at different pH of growth solutions (a) pH = 6.75 and (b) pH = 7.25 deposited on steel substrate coated with a thin film of PS-P4VP. (c) Cyclic voltammogram of gold nanoflowers (500 mV/sec, cap 250 µm, 0.1 M Na_2SO_4)

Figure 5c displays two different voltammograms of a stainless steel sample coated with PS-P4VP and covered by two different nanoflowers structures. The morphology of the NFs has been observed by SEM and display in *figures* 5a and b. The NFs morphology is quite similar to an arborescent structure in *figure 5a*, and is more dendritic in *figure 5b*. Voltammograms show a very low signal between -10 mA/cm2 and 10 mA/cm^2. However, the broad large and weak peak at 1 V remains interesting as it might correspond to the oxidation of water into oxygen in the vicinity of the structured sample. The oxidation reaction corresponds to the following equation 1:

$$H_2O \rightarrow O_2 + 4\,H^+ + 4\,e^-$$

$$2\,H^+ + 2\,e^- \rightarrow H_2$$

Equation 1 : Oxydation reaction of water into oxygen (a) and reduction reaction of hydrogen into dihydrogen (b).

Unfortunately, no other peak is visible on the voltamperogram. The only result we could extract from these preliminary measurements is that both electrochemical and optical responses were not satisfying in absence of NFs like structures. Indeed, we could have observed strong electrochemical and optical responses on Au NFs structures and we should expect the same behavior for Au flower-like structures. Additional optical and electrochemical measurements are on the way to be performed on some more well-defined Au structured samples presenting well-defined dendritic morphologies.

4. CONCLUSIONS

In the present paper, we have demonstrated a seed-assisted solution phase route to create large scale gold crystals arrays, having various morphology (flower, aggregates...) in the range of μm with controllable lengths. The use of multistep aqueous chemical process and, particularly a seeded-growth to synthesize nanostructures, represents an applicable technology to create functional materials and, therefore may contribute to the development of efficient nanomaterials for direct sensor applications.

First, in the sequential growth, large-scale hexagonally ordered Au seeds were successfully synthesized by use of soft template. Then, the spatially arranged gold arrays were used for a growth of pattern-arranged Au NFs. Control over the lateral dimensions of these metallic crystal arrays could be achieved by varying the reaction conditions and, particularly the pH of the growth solution. The underlying NFs growth mechanism was also discussed in relation to the chlorine content in the growth solution. However, some questions still remain to be addressed in future studies in order to gain control and reliability. Nonetheless, hierarchical Au NFs with controllable morphology could be fabricated by optimizing the growth solution pH. Finally, in this contribution, we have also characterized the optical properties of these anisotropic NFs. The study has suggested that SERS signals of the probe molecule were directly related to the shape of the Au crystals. Preliminary electrochemical results have shown a need to increase the NFs density and morphology to enhance the electrical response of the substrate.

To take full advantage of these NP-based materials, one of the pre-requisite is the capability of synthesizing the NPs building blocks with controlled dimensions, morphologies, compositions, and reliable functionalities at large scale. With the improved understanding and concomitant control, stepwise solution-phase growth methods should provide effective and powerful fabrication processes for assembling complex nanostructured films, and particularly in the domain of sensor applications.

5. REFERENCES

[1] F. Zhang, G.B. Braun, Y.F. Shi, Y.C. Zhang, X.H. Sun, N.O. Reich, D.Y. Zhao, G. Stucky, Journal of American Chemical Society 132 (2010) 2850-2851.
[2] G-C. Yi, C. Wang, W.I. Park, Semiconductor Science and Technology 20 (2005) S22-S34.
[3] Z.Q. Tian, B. Ren, J-F. Li, Z.L. Yang, Chemical Communication 34 (2007) 3514-3534.
[4] S. Park, S. Kim, W.I. Lee, K-K. Kim, C. Lee, Journal of Nanotechnology 5 (2014) 1836-1841.
[5] H. Chen, X. Kou, Z. Yang, W. Ni, J. Wang, Langmuir 24 (10) (2008) 5233-5237.
[6] X.Y. Dong, X.H. Ji, H.L. Wu, L.L. Zhao, J. Li, W.S. Yang, J. of Phys. Chem. C 113 (2009) 6573-6576.
[7] A. Stojanovic, S. Oliveira, M. Fisher, S. Seeger, Chemistry of Materials 25 (2013) 2787-2792.
[8] S.H. Chen, D.L. Carroll, Journal of Physical Chemistry B 108 (18) (2004) 5500-5506.
[9] W.X. Niu, Z.Y. Li, L.H. Shi, X.Q. Liu, H.J. Li, S. Han, J. Chen, G.B. Xu, Crystal Growth and Design 8 (2008) 4440-4444.

[10] N.R. Jana, L. Gearheart, C.J. Murphy, Chemical Communication 7 (2001) 617-618.
[11] B.I. Kharisov, Recent Patents on Nanotechnologiy 2 (3) (2008) 190-200.
[12] W. Ye, J. Yan, Q. Ye, F. Zhou, Journal of Physical Chemistry C 114 (37) (2010) 15617-15624.
[13] L. Wang, G. Wei, C. Guo, L. Sun, Y. Sun, Y. Song, T. Yang, Z. Li, Colloids and Surfaces A 312 (2008) 148-153.
[14] T. Huang, F. Meng, L. Qi, Langmuir 26 (10) (2010) 7582-7589.
[15] M. Pan, S. Xing, T. Sun, W. Zhou, M. Sindoro, H.H. Teo, Q. Yan, H. Chen, Chemical Communication 46 (38) (2010) 7112-7114.
[16] X-L. Tang, P. Jiang, G-L. Ge, M. Tsuji, S-S. Xie, Y-J. Guo, Langmuir 24 (5) (2008) 1763-1768.
[17] J. Zhang, L. Meng, D. Zhao, Z. Fei, Q. Lu, P.J. Dyson, Langmuir 24 (6) (2008) 2699-2704.
[18] Z. Wang, M. Bharathi, R. Hariharaputran, H. Xing, L. Tang, J. Li, Y-W. Zhang, Y. Lu, ACS nano7 (2013) 2258-2265.
[19] Y. Liu, K.B. Male, P. Bouvrette, J.H.T. Luong, Chemistry of Materials 15 (22) (2003) 4172-4180.
[20] J-L. Lee, K. Kamada, N. Enomoto, J. Hojo, Chemistry Letters 36 (2007) 728-729.
[21] D. Huang, X. Bai, L. Zheng, Journal of Physical Chemistry C 115 (30) (2011) 14641-14647.
[24] J.P Spatz, S. Mossner, C. Hartmann, M. Möller, Langmuir 16 (2) (2000) 407-415.
[25] C-H. Yu, Y-H Chuang, S-H. Tung, Polymer 52 (18) (2011) 3994-4000.
[28] X. Zhang, Q. Zhou, W. Wang, L. Shen, Z. Li, Z. Zhang, Materials Research Bulletin 47 (3) (2012) 921-924.
[29] L. Jiang, W. Wang, H. Fuchs, L. Chi, Small 5 (24) (2009) 2819-2822.
[30] J. Huang, X. Han, D. Wang, D. Liu, T. You, ACS Applied Materials and Interfaces 5 (18) (2013) 9148-9154.
[31] Q. Lu, J. Zhang, X. Liu, Y. Wu, R. Yuan, S. Chen, Royal Society of Chemistry 139 (2014) 6556-6562.
[32] S.K. Youn, N. Ramgir, C. Wang, K. Subannajui, V. Cimalla, M. Zacharias, Journal of Physical Chemistry C 114 (22) (2010) 10092-10100.
[33] T.H. Kim, J. Huh, J. Hwang, H-C. Kim, S-H. Kim, B-H. Sohn, C. Park, Macromolecules 42 (2009) 6688-6697.
[34] L. Zhao, X. Ji, X. Sun, J. Li, W. Yang, X. Peng, Journal of Physical Chemistry C 113 (38) (2009) 16645-16651.
[35] J. Jiu, K. Murai, D. Kim, K. Kim, K. Suganuma, Preparation of Ag nanorods with high yield by polyol process, Materials Chemistry and Physics 114 (2009) 333-338.

(Article reçu le 01/10/2015, sous forme définitive le 07/01/2016).